

A HYBRID MULTIMODE CONTOUR INTEGRAL METHOD FOR ANALYSIS OF THE H -PLANE WAVEGUIDE DISCONTINUITIES

A. Banai

School of Electrical Engineering
Sharif University of Technology
Tehran, Iran

A. Hashemi

Faculty of Engineering
Islamic Azad University
Science & Research Campus, Tehran, Iran

Abstract—A hybrid method is introduced for analysis of the H -plane waveguide discontinuities. It combines multimode contour integral and mode matching techniques. The process is based on dividing the circuit structure into key building blocks and finding the multimode scattering matrix of each block individually. The multimode scattering matrix of the whole structure can be found by cascading these blocks. Also contour integral method is developed for analysis of multi-media circuits. Therefore, it is possible to analyze H -plane waveguide filters with dielectric resonators using this method. The accuracy and run time of the proposed method is compared with those reported in literatures and/or Ansoft HFSS software.

1. INTRODUCTION

H -plane rectangular waveguide circuits consist of inductive obstacles and discontinuities are the key elements of many microwave circuits and devices. The correct analysis and design of these circuits is of great importance for many applications such as satellite and wireless communication systems [1–4].

There are three main categories of methods for the analysis of the microwave circuits:

- analytical or modal methods;
- numerical methods;
- hybrid methods.

The analytical methods can give good solutions with reasonable CPU time for only waveguide problems with regular shapes. The numerical methods are capable of analyzing any waveguide problem with arbitrary shape, but need a lot of CPU time and memory. The aim of hybrid methods is the combination of the main advantages of other techniques. They combine the efficiency and accuracy of analytical methods and the flexibility of numerical methods. Compared with numerical methods, hybrid methods are more accurate and reduce the CPU time and the storage requirements.

A great number of hybrid techniques have been reported over the last years, with an increasing degree of flexibility [5–11].

This article presents a hybrid method based on multimode contour integral and mode matching techniques. It is capable of analyzing the H -plane discontinuities in a rectangular waveguide. The process is based on segmentation and dividing the structure into key building blocks. We use the multimode contour integral method to analyze the blocks including irregular shape inductive discontinuities or dielectric discontinuities. In opposite to traditional contour integral method, which considers only the effect of dominant mode (TE_{10}) on wave ports, multimode contour integral considers the effect of higher order modes (TE_{n0}) excited by discontinuities on these ports. The mode matching technique will be used to analyze the blocks which can be easily treated by modal expansion. Finally, the multimode scattering matrix of the whole structure can be found by cascading the blocks. Therefore, the new method is suitable for analysis of a wide range of waveguide problems.

In the following sections, in Section 2 we describe the basis of contour integral method and develop it to include the effect of higher order modes and analysis of multi-media problems. In Section 3, we describe the purposed hybrid method. Section 4 provides the simulated results and finally, Section 5 concludes the paper.

2. BASIS OF CONTOUR INTEGRAL METHOD

The contour integral (CI) method is one of the planar circuit analysis methods [12–15]. Consider an arbitrary shaped planar circuit having coupling (or wave) ports, such as shown in Fig. 1. From the Maxwell's equation, it is found that the RF voltage in region D satisfies the two-

dimensional wave equation [14]:

$$(\nabla^2 + k^2) V = 0 \tag{1}$$

where $k = \omega\sqrt{\mu\varepsilon}$ denotes the wave-number in medium.

However, when we are concerned only with the voltage along the periphery, the wave equation can be converted into a contour integral form, which relates the voltage and current along the circuit periphery [13]. Using Weber’s solution for cylindrical waves, the RF voltage at a point upon the periphery is given as [13]:

$$V(s) = \frac{1}{j4} \oint_C \left\{ k \cos \theta H_1^{(2)}(kr) V(s_0) - j\omega\mu b H_0^{(2)}(kr) J(kr) \right\} ds_0 \tag{2}$$

In this equation, $H_0^{(2)}$ and $H_1^{(2)}$ are the zeroth-order and first-order Hankel functions of the second kind, respectively. The variable r denotes distance between points (s) and (s_0), θ is the angle between the line passes through s and s_0 and the normal to the periphery at (s_0), J denotes the current density flowing outwards along the periphery, and b the height of the circuit.

To solve (2) numerically, the circuit’s periphery is divided into N sub-ports numbered as 1, 2, \dots , N having width W_1, W_2, \dots, W_N , respectively, as illustrated in Fig. 1. By finding the midpoint of each sub-port, we create N sampling points. When we assume that the magnetic and electric field intensities are constant over each sub-ports, (2) results in a system of matrix equations [14]:

$$\sum_{n=1}^N u_{mn} V_n = \sum_{n=1}^N h_{mn} I_n \quad \text{or} \quad [U]_{N \times N} (V_S)_N = [H]_{N \times N} (I_S)_N \tag{3}$$

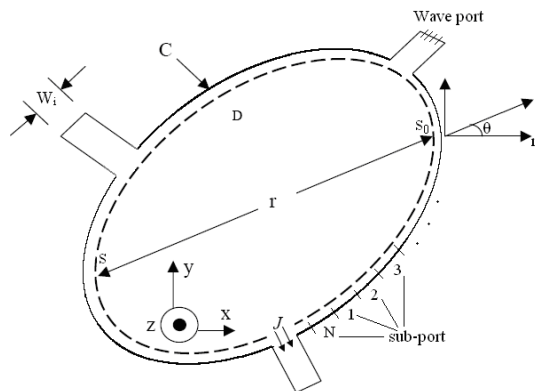


Figure 1. Typical planar circuit and symbols used in (2).

where

$$u_{mn} = \delta_{mn} - \frac{k}{j2} \int_{W_n} \cos \theta H_1^{(2)}(kr) ds, \quad \delta_{mn} \begin{cases} 1; & (m = n) \\ 0; & (m \neq n) \end{cases}$$

$$h_{mn} = \begin{cases} \frac{\omega \mu b}{4} \frac{1}{W_n} \int_{W_n} H_0^{(2)}(kr) ds; & (m \neq n) \\ \frac{\omega \mu b}{4} \left[1 - \frac{j2}{\pi} \left(\ln \frac{kW_m}{4} - 1 + \gamma \right) \right]; & (m = n) \end{cases} \quad (4)$$

$\gamma = 0.5772 \dots$ is Euler's constant, and $I_n = -2JW_n$ represents the total current flowing into the n -th port on both the upper and lower surfaces of the circuit plate.

Solving (3), the RF voltage on each sampling point is obtained as:

$$(V_S) = [U]^{-1} [H] (I_S) \quad (5)$$

The CI method is also applicable for analyzing the rectangular waveguide circuits that have not any changes in one dimension in which the TE_{n0} modes are excited [14–16]. Consider an H -plane waveguide coupled circuit as shown in Fig. 2. The periphery of the circuit is again divided and numbered as follows:

Input port: $i = 1 \sim m$

Output port: $i = (m + 1) \sim (m + n)$

Circuit periphery: $i = (m + n + 1) \sim (m + n + L)$

Thus $m + n + L (= N)$ sub-ports (or sampling points) are provided.

The derivation of the matrix equation, such as (3), follows entirely the same process as described in above.

In the following subsections, at first we describe conventional application of CI method in waveguide circuit analysis. Next, two new versions of CI methods are discussed.

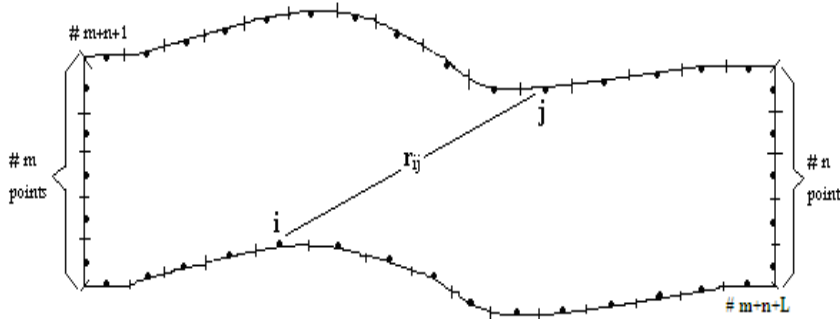


Figure 2. Typical H -plane waveguide circuit.

2.1. Single-mode CI Method

In conventional applications of the CI method to solve waveguide problems, we interest to deal with the characteristics of only dominant propagating mode (TE₁₀) on reference planes. Thus, the straight waveguide sections with appropriate length (almost $\lambda/2$) are added in both sides of reference planes [14–16]. It is caused the effect of non-propagating higher order modes (TE_{*n*0}), which excited by discontinuities, can be neglected on these reference planes. Thus, it can be named single mode CI method.

Applying the short circuit condition of peripheral sub-ports for the admittance matrix of N sub-ports, $[Y_T] = [H]^{-1}[U]$, results in the admittance matrix of wave ports named $[Y]$. Finally, the scattering matrix of wave ports can be found as:

$$[S] = (Y_0 [E] + [Y])^{-1} (Y_0 [E] - [Y]) \quad (6)$$

where $[E]$ represents the identity matrix and Y_0 is the waveguide admittance in TE₁₀ mode and calculated as [14–18]:

$$\frac{1}{Y_0} = Z_0 = 120\pi \frac{b}{a} \frac{1}{\sqrt{1 - (\lambda/2a)^2}} = \frac{b}{a} Z_{\text{TE}_{10}} \quad (7)$$

In this equation, “ a ” and “ b ” are the width and height of waveguide cross section, respectively. λ is the wavelength in free space and $Z_{\text{TE}_{10}}$ is the wave impedance of TE₁₀ mode.

2.2. Multimode CI Method

In single mode CI method, the presence of straight waveguide sections on both sides of the reference planes increase the size of the circuit and, therefore, the number of sub-ports on the boundary which all lead to higher computational costs. Also, it is not reasonable to ignore the effect of higher order modes since distances between the existing discontinuities and wave ports are small. In this case, for having more accurate results, it is necessary to evaluate the generalized scattering matrix (GSM) of the circuit because the complex power flow into the evanescent modes on either side of the discontinuity is considerable.

For all the above reasons, the multimode CI method is introduced. This method, at first, was introduced by Okoshi [14], but up to our knowledge, it has not been yet applied to waveguide circuit analysis. In multimode CI method we consider that at each reference plane ($M-1$) higher order TE modes (TE₂₀, TE₃₀, . . . , TE_{*M*0}) exist in addition to the fundamental TE₁₀ mode.

We set the x coordinate along the reference plane. We denote the spatial peak voltage and current density of the n -th mode by V_{pn} and J_{pn} , respectively. Then the voltage and current density of the n -th mode at x are expressed as:

$$\begin{aligned} v_n(x) &= V_{pn} \sin\left(\frac{n\pi}{a}x\right) \\ j_n(x) &= J_{pn} \sin\left(\frac{n\pi}{a}x\right) \end{aligned} \quad (8)$$

The voltage and current of each sub-port, on reference plane, can be written as a linear combination of voltages and currents of different modes, respectively:

$$\begin{aligned} (V_S) &= \begin{pmatrix} V_{S_1} \\ \vdots \\ V_{S_M} \end{pmatrix} = \begin{pmatrix} \alpha_{11}V_1 + \cdots + \alpha_{1M}V_M \\ \vdots \\ \alpha_{M1}V_1 + \cdots + \alpha_{MM}V_M \end{pmatrix} = [\alpha](V) \\ (I_S) &= \begin{pmatrix} I_{S_1} \\ \vdots \\ I_{S_M} \end{pmatrix} = \begin{pmatrix} \beta_{11}I_1 + \cdots + \beta_{1M}I_M \\ \vdots \\ \beta_{M1}I_1 + \cdots + \beta_{MM}I_M \end{pmatrix} = [\beta](I) \end{aligned} \quad (9)$$

where V_n and I_n ($n = 1, \dots, M$) denote to voltage and current of TE_{n0} mode, and are defined as:

$$\begin{aligned} V_n &= \frac{1}{a/n} \int_0^{a/n} V_{pn} \sin\left(\frac{n\pi}{a}x\right) dx \\ I_n &= \int_0^{a/n} J_{pn} \sin\left(\frac{n\pi}{a}x\right) dx \end{aligned} \quad (10)$$

The elements of coefficient matrices, $[\alpha]$ and $[\beta]$, are defined as:

$$\begin{aligned} \alpha_{mn} &= \frac{M}{n} \sin\left(\frac{2m-1}{2M}n\pi\right) \sin\left(\frac{n\pi}{2M}\right) \\ \beta_{mn} &= \sin\left(\frac{2m-1}{2M}n\pi\right) \sin\left(\frac{n\pi}{2M}\right) \end{aligned} \quad m, n = 1, \dots, M \quad (11)$$

On reference planes, the higher order modes are evanescent and only the dominant mode (TE_{10}) propagates. Therefore, we assume that the higher order modes are terminated with their reactive characteristic impedances [14]:

$$Z_{n0} = \frac{V_n}{I_n} = j 120\pi \frac{b}{a/n} \frac{1}{\sqrt{(n\lambda/2a)^2 - 1}} \quad (12)$$

Similar reasoning of the single-mode CI method leads to the GSM of the circuit, including the effect of higher order modes.

2.3. Analysis of Multi-media Problems

For multi-media cases, any boundary method requires to make up equations for each homogeneous sub-domain constructed of one medium. To do this, consider a general geometry of a two media circuit, as shown in Fig. 3, where regions (I) and (II) are homogeneous sub-domains. We divide each wave port to m and post's periphery to M sub-ports.

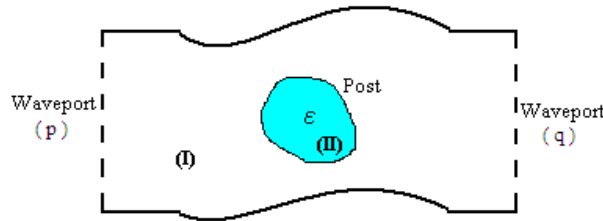


Figure 3. Top view of the H -plane waveguide circuit with a dielectric post.

Rewriting (3) for region (I) gives:

$$[U_I] \begin{pmatrix} (V^p) \\ (V^q) \\ (V_I^{Post}) \\ (0) \end{pmatrix} = [H_I] \begin{pmatrix} (I^p) \\ (I^q) \\ (I_I^{Post}) \\ (I^{sc}) \end{pmatrix}; \quad \text{on } C_1 + C_2 \quad (13)$$

In (13) the superscripts p , q , $Post$, and sc denote to sub-ports located on wave ports named p and q , post's boundary, and short circuit sections of contour, respectively. In the same manner, we can write (3) for region (II):

$$[U_{II}] (V_{II}^{Post}) = [H_{II}] (I_{II}^{Post}); \quad \text{on } C_2 \quad (14)$$

The boundary conditions on the interface are as follows:

$$\begin{aligned} (V_{II}^{Post}) &= (V_I^{Post}) = (V^{Post}) \\ (I_{II}^{Post}) &= - (I_I^{Post}) = - (I^{Post}) \end{aligned} \quad (15)$$

The minus sign in current boundary condition originated from the outward normal directions of the adjacent two sub-regions opposite each other, as shown in Fig. 4.

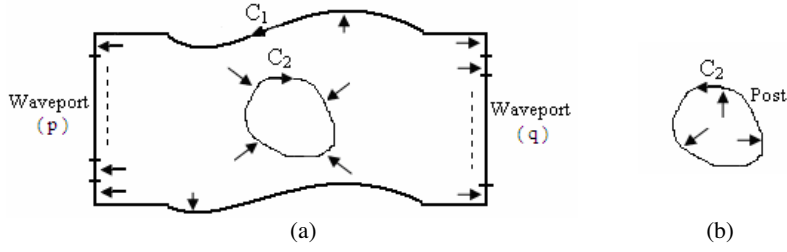


Figure 4. Current direction in sub-ports on boundary of regions, (a) region I, (b) region II.

The main goal in CI method is determination of relation among voltages and currents on wave ports, i.e., the relation between (V^p) and (V^q) with (I^p) and (I^q) . Thus, from (14) and (15) we obtain:

$$(V^{Post}) = -[U_{II}]^{-1}[H_{II}](I^{Post}) = -[Z^{Post}](I^{Post}) \quad (16)$$

The matrix $[Z^{Post}]$ is the impedance matrix of post. Replacing (16) in (13) results in:

$$\begin{pmatrix} (I^p) \\ (I^q) \\ (I^{Post}) \\ \text{---} \\ (I^{sc}) \end{pmatrix} = [Y_I] \begin{pmatrix} (V^p) \\ (V^q) \\ -[Z^{Post}](I^{Post}) \\ \text{---} \\ (0) \end{pmatrix} \quad (17)$$

where $[Y_I]$, the sub-ports admittance matrix of region (I), is defined as:

$$[Y_I] = [H_I]^{-1}[U_I] \quad (18)$$

We write $[Y_I]$ as below [19]:

$$\left[\begin{array}{ccc|c} \left[\begin{array}{ccc} [Y_I^{p,p}] & [Y_I^{p,q}] & [Y_I^{p,Post}] \\ [Y_I^{q,p}] & [Y_I^{q,q}] & [Y_I^{q,Post}] \\ [Y_I^{Post,p}] & [Y_I^{Post,q}] & [Y_I^{Post,Post}] \end{array} \right]_{(M+2m) \times (M+2m)} & & & \\ \hline & & & \end{array} \right]_{N \times N} \quad (19)$$

The sizes of sub-matrices of $[Y_I]$ depend on the number of sub-ports on wave ports and around the post. Finally, by using these sub-matrices we find the final relations among currents and voltages as below:

$$\begin{aligned}
 (I^p) &= \left\{ [Y_I^{p,p}] - [C^p][A][Y_I^{Post,p}] \right\} (V^p) \\
 &\quad + \left\{ [Y_I^{p,q}] - [C^p][A][Y_I^{Post,q}] \right\} (V^q) \\
 (I^q) &= \left\{ [Y_I^{q,p}] - [C^q][A][Y_I^{Post,p}] \right\} (V^p) \\
 &\quad + \left\{ [Y_I^{q,q}] - [C^q][A][Y_I^{Post,q}] \right\} (V^q)
 \end{aligned} \tag{20}$$

In this equation, the coefficient matrices are defined as below:

$$\begin{aligned}
 [C^p] &= [Y_I^{p,Post}] [Z^{Post}]; \quad [C^q] = [Y_I^{q,Post}] [Z^{Post}] \\
 [A] &= \{ [E] + [C^{Post}] \}^{-1} \\
 [E] &= \text{unit matrix}; \quad [C^{Post}] = [Y_I^{Post,Post}] [Z^{Post}]
 \end{aligned} \tag{21}$$

By using (13), it is easy to find other characteristics of circuit such as scattering matrix or impedance matrix [14–18].

3. OUR PURPOSED HYBRID METHOD

Consider a waveguide circuit containing some arbitrary shape H -plane discontinuities. Specially, if these discontinuities are due to dielectric posts or slabs, the use of CI method for analysis of whole structure needs too many sub-ports. This leads to increment of the size of matrices in CI method and finally, raise the computational costs. Also, this matrices enlargement, increase the possibility of singularity in them. It can cause to reduce the accuracy of results.

To solve this type of circuits, hybrid methods are suggested. In this section, a new hybrid method is introduced. It combines contour integral and mode matching techniques. The main goal in our purposed hybrid method is determination of the multimode scattering matrix of the circuit.

To introduce the purposed method, consider Fig. 5(a) that shows an H -plane waveguide circuit including some discontinuities. We divide the circuit into key building blocks, as shown in Fig. 5(b). Some of these blocks contain irregular shape discontinuities. These blocks are analyzed with contour integral method. It is obvious that the single-mode CI method is not applicable because there

are not straight waveguide sections in both side of discontinuity. Therefore, the multimode CI method, which considers the effect of higher order modes, must be used. The blocks consist of regular shape discontinuities are analyzed with mode matching method. After obtaining the GSM of all blocks, the GSM of whole structure can be found by cascading these GSMs.

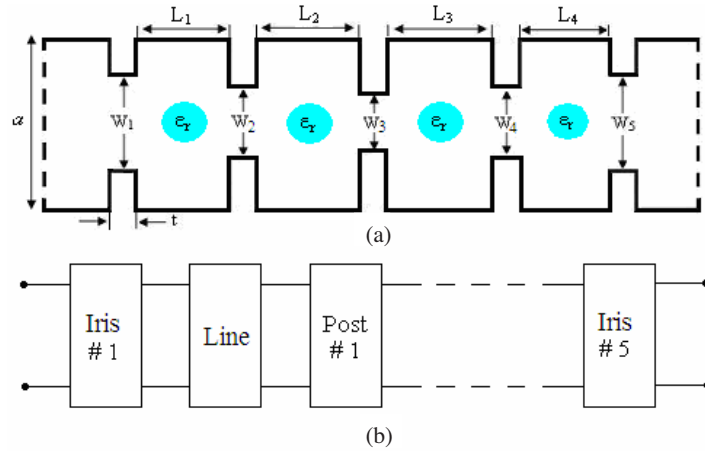


Figure 5. An H -plane waveguide circuit including some discontinuities, (a) top view of the structure, (b) key building blocks of the structure.

4. SIMULATION RESULTS

In order to compare the results of abovementioned our methods with others, we analyze some H -plane rectangular waveguide circuits.

The first example compares the single mode and multi-mode CI methods. We obtain the S parameters of the circuit by these methods. The Ansoft HFSS software is used to verify the results.

Consider a waveguide circuit including a metallic circular post. The post radius is $r = 1$ millimeter and locates in the center of WR-90 waveguide. Geometry of the circuit is shown in Fig. 6(a).

To compare these methods, in the first case, we consider the straight waveguide sections with suitable length in both side of the post. Because the post is far from the wave ports, the effect of non-propagating higher order TE_{n0} modes, excited by discontinuity, can be neglected on these ports. Thus, in this case, both methods have high accuracy as shown in Fig. 6(b) and multimode CI has not any advantages over single-mode CI method.

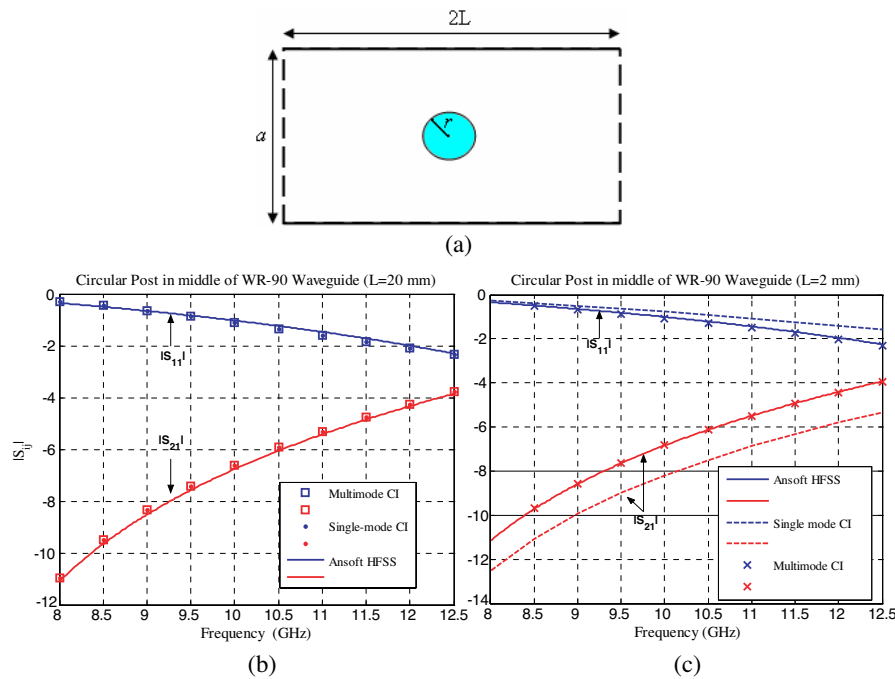


Figure 6. Analysis of circular post discontinuity in rectangular waveguide for comparison of single-mode and multimode contour integral methods, (a) geometry of circuit, (b) S parameters in the case of $L = 10$ mm, (c) S parameters in the case of $L = 2$ mm.

In the second case, we place the wave ports near the post. In this case, the magnitudes of non-propagating higher order modes are considerable and neglecting them in single-mode CI method leads to error. This problem is shown in Fig. 6(c).

In the second example, an H -plane direct-coupled-cavities filter with dielectric resonators (DR) has been analyzed. Fig. 5, in previous section, shows the circuit structure and its key building blocks.

Waveguide used in this filter is WR-75 with cross section 19.05×9.525 . The irises have the thickness equal to $t = 2$. The width of diaphragms are $W_1 = W_5 = 13.37$, $W_2 = W_4 = 6.286$, and $W_3 = 6.1$. The length of resonators are $L_1 = L_4 = 6.98$, and $L_2 = L_3 = 8.28$. The radius of DRs are $r_1 = r_4 = 2.111$, and $r_2 = r_3 = 2.172$ (All sizes are in millimeter.) and have dielectric constant equal to $\epsilon_r = 24$.

For analyzing the whole structure using the single mode CI method, we divide the boundary of each post to 180 sub-ports and

the total sub-port number is 940. For analyzing this filter using our proposed hybrid method, the blocks including DR are analyzed with multimode CI method, whereas the blocks including irises are analyzed with mode matching technique. Using this method, we achieve higher accuracy as depicted in Fig. 7. Also, in this figure, we compare our results with those reported in [20].

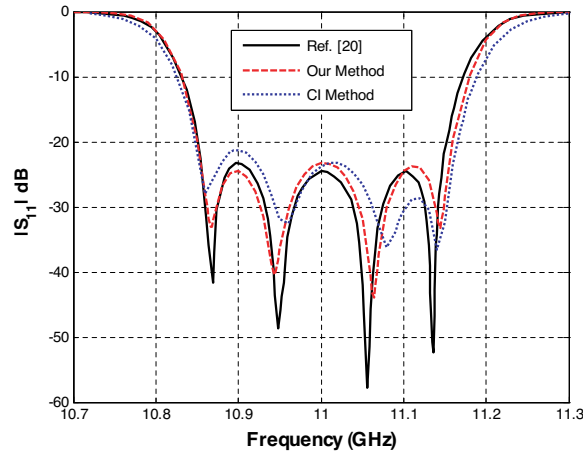


Figure 7. The S_{11} parameter of the filter shown in Fig. 5.

Other advantages of the hybrid method over CI method are due to reduce the size of matrices in hybrid method. The number of sub-ports in DR blocks that was analyzed with multimode CI method is 220. This size reduction results in less memory usage. Also it makes more well-conditioned matrices as the reciprocal condition number is of order 10^{-3} instead of 10^{-4} . This reduces the possibility of having singular matrices [21].

However, the simulation time in a Pentium IV with CPU 2.4 Celeron for each sample frequency is 36 s for CI method and 6 s for our hybrid method. The simulation time for some commercial software has been reported in [20]. This time is 2 h for CST and 6 h for HFSS software. This enhances the high efficiency of our method.

In the last example, an H -plane evanescent mode waveguide filter loaded with circular dielectric resonators has been analyzed. Fig. 8(a) shows the circuit structure. The height of all the structure is 9.525 mm. The widths of the input and output waveguides are fixed to 19.05 mm (standard WR-75).

The housing of the filter is fixed to 8 mm. Again, we divide the circuit into building blocks. The blocks including DRs are analyzed

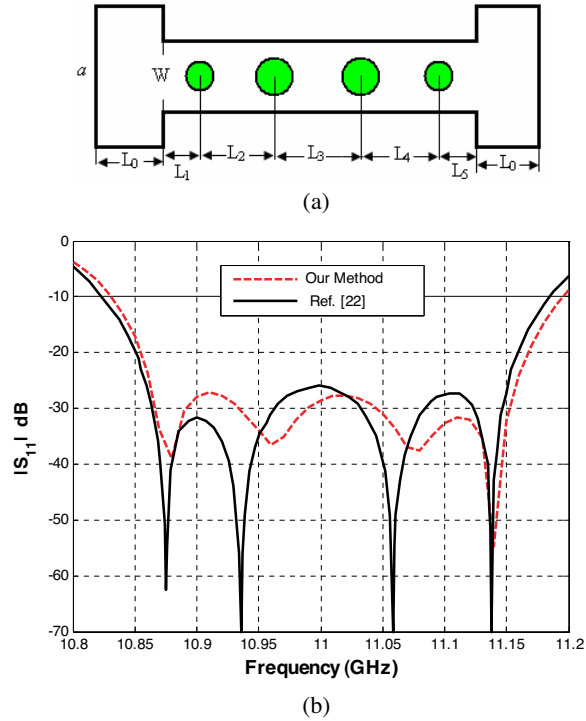


Figure 8. Evanescent mode waveguide bandpass filter with DRs ($\epsilon_r = 24$). (a) Circuit geometry: (All sizes in mm), $a = 19.05$, $W = 8$, $L_1 = L_5 = 2.4179$, $L_2 = L_4 = 10.182$, $L_3 = 10.9919$, DRs radii: $r_1 = r_4 = 0.777$, $r_2 = r_3 = 2.169$, (b) S_{11} parameter of filter.

with multimode CI method, whereas the blocks including steps are analyzed with mode matching technique. Our results compared with those reported in [22] are shown in Fig. 8(b).

5. CONCLUSION

A new hybrid method was introduced for analyzing the H -plane waveguide circuits. In this method a suitable combination of two analysis techniques, multimode contour integral and mode matching, has been used. Also, the contour integral method was developed to analyze the multi-media circuits, specially, full height dielectric posts into the rectangular waveguide circuits. In comparison with other methods and some commercial software, our method is very fast. It provides an efficient tool for the analysis of H -plane waveguide filters

with dielectric resonators in reasonable CPU time. Also, the sizes of matrices produced in the hybrid method are smaller than them in CI method. It makes more well-conditioned matrices and reduces the possibility of singularity in matrices. The accuracy of the hybrid method was validated by comparison of results with those reported in literatures.

ACKNOWLEDGMENT

The authors wish to acknowledge the assistance and support of the Islamic Azad university- Majlesi branch.

REFERENCES

1. Jia, H., K. Yoshtomi, and K. Yasumoto, "Rigorous analysis of rectangular waveguide junctions by Fourier transform technique," *Progress In Electromagnetics Research*, PIER 20, 263–282, 1998.
2. Jia, H., K. Yoshtomi, and K. Yasumoto, "Rigorous analysis of E-/H-plane junctions in rectangular waveguides using Fourier transform technique," *Progress In Electromagnetics Research*, PIER 21, 273–292, 1999.
3. El Sabbagh, M. and K. Zaki, "Modeling of rectangular waveguide junctions containing cylindrical posts," *Progress In Electromagnetics Research*, PIER 33, 299–331, 2001.
4. Lilonga-Boyenga, D., C. N. Mabika, and G. Okoumou-Moko, "Rigorous analysis of uniaxial discontinuities microwave components using a new multimodal variational formulation," *Progress In Electromagnetics Research B*, Vol. 2, 61–71, 2008.
5. Steban, H., S. Cogollos, V. E. Boria, A. San Blas, and M. Ferrando, "A new hybrid mode-matching/numerical method for the analysis of arbitrarily shaped inductive obstacles and discontinuities in rectangular waveguides," *IEEE Trans. Microwave Theory Tech.*, Vol. 50, No. 4, 1219–1224, April 2002.
6. Morro, J. V., P. S. Pacheco, H. E. Gonzalez, V. E. Boria, C. Bachiller, M. Taroncher, S. Cogollos, and B. Gimeno, "Fast automated design of waveguide filters using aggressive space mapping with a new segmentation strategy and a hybrid optimization algorithm," *IEEE Trans. Microwave Theory Tech.*, Vol. 53, No. 4, 1130–1142, April 2005.
7. Xiang, Z. and Y. Lu, "An effective hybrid method for electromagnetic scattering from inhomogeneous objects," *Progress In Electromagnetics Research*, PIER 17, 305–321, 1997.

8. Wu, K. L., G. Y. Delisle, D. G. Fang, and M. Lecours, "Coupled finite element and boundary element methods in electromagnetic scattering," *Progress In Electromagnetics Research*, PIER 02, 113–132, 1990.
9. Nie, X.-C., Y.-B. Gan, N. Yuan, C.-F. Wang, and L.-W. Li, "An efficient hybrid method for analysis of slot arrays enclosed by a large radome," *Journal of Electromagnetic Waves and Applications*, Vol. 20, No. 2, 249–264, 2006.
10. Fikioris, J. G. and A. N. Magoulas, "Scattering from axisymmetric scatterers: A hybrid method of solving Maus's equation," *Progress In Electromagnetics Research*, PIER 25, 131–165, 2000.
11. Liu, H.-X., H. Zhai, L. Li, and C.-H. Liang, "A progressive numerical method combined with MoM for a fast analysis of large waveguide slot antenna array," *Progress In Electromagnetics Research*, PIER 20, No. 2, 183–192, 2006.
12. Mittal, A., K. K. Gupta, G. P. Srivastava, P. K. Singhal, R. D. Gupta, and P. C. Sharma, "Contour integral analysis of planar components," *J. Microwaves and Optoelectronics*, Vol. 3, No. 3, 58–72, Dec. 2003.
13. Okoshi, T. and T. Miyoshi, "The planar circuit — An approach to microwave integrated circuitry," *IEEE Trans. Microwave Theory Tech.*, Vol. 20, No. 4, 245–252, Apr. 1972.
14. Okoshi, T., *Planar Circuits for Microwaves and Lightwaves*, Springer-Verlag, 1985.
15. Itoh, T., Ed., *Numerical Techniques for Microwave and Millimeter-Wave Passive Structures*, Wiley, 1989.
16. Okoshi, T. and S. Kitazawa, "Computer analysis of short-boundary planar circuits," *IEEE Trans. Microwave Theory Tech.*, Vol. 23, No. 3, 299–306, March 1975.
17. Hashemi, A. and A. Banai, "Analysis of H-plane waveguide discontinuities using hybrid multimode contour integral and mode matching techniques," *2007 SBMO/IEEE MTT-S (IMOC2007)*, 840–843, 2007.
18. Hiraoka, T. and J. P. Hsu, "Equivalent network for H-plane rectangular waveguide circuits and its practical application for analysis of circuit performance and field behavior," *Int. J. RF and Microwave CAE*, Vol. 14, No. 3, 210–226, Wiley Interscience, April 2004.
19. Hashemi, A. and A. Banai, "Analysis of waveguide filters with dielectric resonators using multimode contour integral method," *2007 IEEE MTT-S (APMC2007)*, 2083–2086, 2007.

20. Bachiller, C., H. Esteban, V. E. Boria, J. V. Morro, L. J. Rogla, M. Taroncher, and A. Belenguer, "Efficient CAD tool of direct-coupled-cavities filters with dielectric resonators," *2005 IEEE AP-S*, Vol. 1B, 578–581, 2007.
21. Qiu, Z.-J., X.-Y. Hou, X. Li, and J.-D. Xu, "On the condition number of matrices from various hybrid vector FEM-BEM formulations for 3-D scattering," *Journal of Electromagnetic Waves and Applications*, Vol. 20, No. 13, 1797–1806, 2006.
22. Bachiller, C., H. Esteban, V. E. Boria, J. V. Morro, M. Taroncher, and B. Gimeno, "CAD of evanescent mode waveguide filters with circular dielectric resonators," *2006 IEEE AP-S*, 1567–1570, 2006.